J Electroceram (2006) 16:499–502
DOI 10.1007/s10832-006-9905-1

Mesophase configurations and optical properties of mesoporous TiO_2 thin films

Yu Zhang · John Wang · Jun Li

Abstract Highly ordered mesoporous TiO_2 thin films have been successfully synthesized via a copolymer templating sol-gel route. A configuration transition from hexagonal, to cubic, and then to a channel-like structure was observed when the copolymer-templated thin film was thermally annealed from 110 to 450°C. In the mesoporous TiO_2 film annealed at 450°C, mesopores were merged in a preferential direction, forming a channel-like structure consisting of a semicrystalline (anatase) framework. These films exhibit excellent optical transparency with transmittance higher than 85% in the visible region. A blue shift in UV-Vis absorption onset was shown for the mesoporous TiO_2 films, indicating a size quantization effect of nanocrystalline titania.

Keywords Mesoporous thin film · Titania · Mesophase configuration · Optical properties

1 Introduction

Mesoporous materials have attracted much attention, since the discovery of mesoporous aluminosilicates in the early 1990s [1]. They exhibit an extra high specific surface area, together with a diversity in pore configuration, including for example, hexagonal (MCM-41), cubic (MCM-48), and lamellar (MCM-50) mesostructures [2]. Several other mesostructures, such as SBA-1, SBA-2, SBA-3 have also been reported [3–5]. Obviously, these previous studies on mesostructures were largely devoted to silica-based compositions, whereby they were well defined with stable amorphous structures. In contrast, much less work has been done with TiO_2-based mesoporous structures [6, 7], although they have demonstrated excellent functional properties for various advanced applications, such as in solar energy conversion [8–10], batteries [11] and photocatalysis [12].

Indeed, Ti-alkoxide chemistry is rather complex, where a delicate balance between hydrolysis and condensation reactions is difficult to control. In addition, the metal-oxo polymeric groups involved tend to undergo crystallization in an uncontrolled manner upon thermal annealing [13], attributing to the subtlety of pore arrangement for TiO_2-based mesoporous structures. While a typical mesoporous TiO_2 film consists of three constituent phases, including pores, amorphous titania and nanocrystalline anatase phase, the mesopore configuration can undergo a steady change with a number of parameters involved in the copolymer templating and subsequent thermal annealing processes. In this paper, we report a study on the effects of thermal anneal temperature (110°C–450°C) on the mesophase configurations in TiO_2 thin films derived from copolymer templating. The optical properties of these mesoporous TiO_2 thin films are also investigated.

2 Experimental procedure

Mesoporous TiO_2 thin films were synthesized at room temperature by following the procedures detailed below: a precursor solution was prepared by mixing appropriate amounts of ethanol, hydrochloric acid (HCl), titanium tetra-isopropoxide (TTIP, Aldrich, 97%), acetyl acetone (AcAc) and deionized water (H_2O), which was stirred for two hours. An appropriate amount of triblock

Y. Zhang · J. Wang (✉)
Department of Materials Science and Engineering, Faculty of Engineering, National University of Singapore, Singapore 117576
e-mail: msewangj@nus.edu.sg

J. Li
Division of Bioengineering & IMRE, Faculty of Engineering, National University of Singapore, Singapore 117576

copolymer Pluronic F127 (designated $EO_{106}PO_{70}EO_{106}$, BASF) was dissolved in ethanol and then mixed with the precursor solution. Molar ratios of these ingredients were controlled at: TTIP/F127/AcAc/HCl/H_2O/ethanol = 1:0.005:0.5:0.5:15:40. Upon stirring for three more hours, the sol solution was deposited on glass substrates by spin coating (3000 rpm for 1 min). A gentle heating was then applied to enhance the inorganic polymerization and stabilize the mesophases, typically at 40°C (for 48 h) and then 110°C (for 24 h) in air. They were then thermally annealed in air at 350°C (for 4 h). Further thermal annealing at 450°C (for 1 h) was performed, in order to improve the nanocrystallinity of the mesoporous TiO_2 thin film. The heating rate for all the thermal annealing treatment was controlled at a 1°C min^{-1} ramp.

Both TEM (JEOL JEM 2010F, 200 kV) and high resolution TEM (HRTEM, JEOL JEM 3010, 300 kV) were employed to study the morphology and texture of the mesoporous TiO_2 films. The nanocrystallites of anatase phase in the mesoporous thin films were characterized using Raman spectrometer (U1000 Jobin-Yvon double monochromator). Their optical properties were measured using a UV-visible spectrophotometer (UV-1601, Shimadzu).

3 Results and discussion

Temperature is an important variable that strongly affect the mesostructures of thin films derived from copolymer templating. As shown in Fig. 1(a), the mesostructure exhibited a hexagonal configuration, when the film was first thermally annealed at 110°C, where the ordered arrays were aligned more or less parallel to the substrate surface. It consisted of self-assembled copolymer and precursor phase for TiO_2. Upon thermal annealing at 350°C (Fig. 1(b)), the copolymer template was removed from the mesostructure. The resulting pore arrays exhibit a cubic morphology. When the mesoporous film was further thermally annealed at 450°C, the pores tended to merge to form a channel-like structure (Fig. 1(c)). Selected area electron diffraction pattern (Fig. 1(d)) consisted of several weak rings, revealing that the mesoporous TiO_2 film annealed at 450°C was partially crystallized. Further studies using HRTEM confirmed the occurrence of fine anatase crystallites in the film, upon thermal annealing at 450°C (Fig. 1(e)).

To further confirm the nanocrystalline anatase structure for the mesoporous thin film, Fig. 2 shows the Raman spectra for the thin film samples thermally annealed at 110, 350 and 450°C, respectively. There is no any apparent nanocrystalline phase in the film thermally annealed at 110°C. Similarly, only one broadened band at around 100 to 200 cm^{-1} is shown for the film thermally annealed at 350°C. In contrast, three well established bands at 399, 519 and 638 cm^{-1}, which are characteristic of anatase phase [14], are shown for the mesoporous TiO_2 film thermally annealed at 450°C, confirming the occurrence of anatase nanocrystallites.

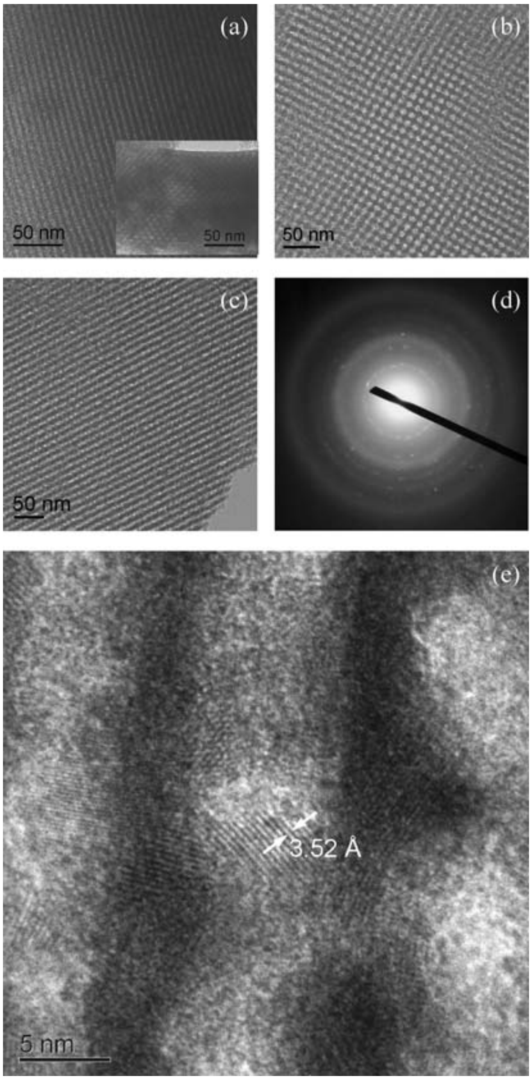

Fig. 1 TEM micrographs of TiO_2 thin films derived from copolymer templating, upon thermal annealing at (a) 110°C, (b) 350°C, (c) 450°C, (d) SAD pattern of (c), (e) HRTEM image of (c)

UV-vis spectroscopy was employed to characterize the optical behaviors and electronic structure of the mesoporous TiO_2 thin films. Shown in Fig. 3 are the transmittance spectra of the thin film samples thermally annealed at 110°C, 350°C and 450°C, respectively. They are all of optical transparency with transmittance higher than 85% in the visible region. The sharp decrease in transmittance at around 360 nm is related to the semiconductor bandgap of TiO_2, where electrons are excited from valence band to conduction band. The shift in the band edges (as compared to 380 nm for bulk anatase) is a result of the much refined sizes of nanocrystallites in the mesoporous TiO_2 thin films.

The absorption edge of the mesoporous TiO_2 thin films shows a slight "red shift" with increasing thermal annealing

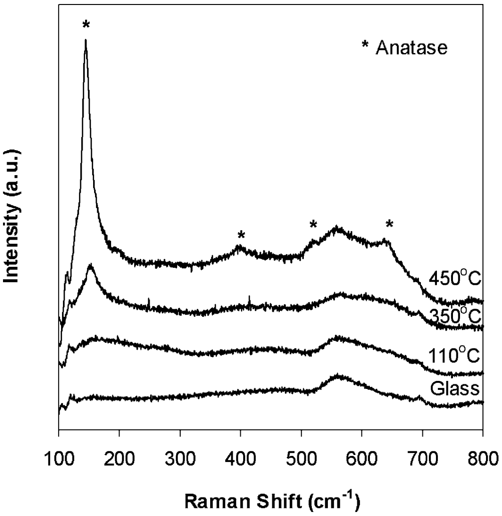

Fig. 2 Raman spectra of TiO_2 thin films derived from copolymer templating, upon thermal annealing at 110°C, 350°C and 450°C, respectively

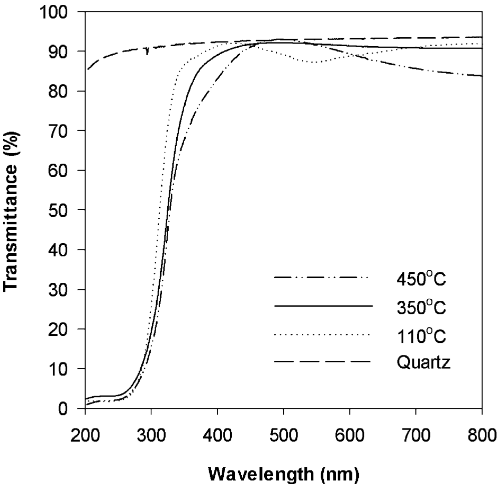

Fig. 3 UV-vis transmittance spectra of the TiO_2 thin films derived from copolymer templating and then thermally annealed at 110°C, 350°C and 450°C, respectively

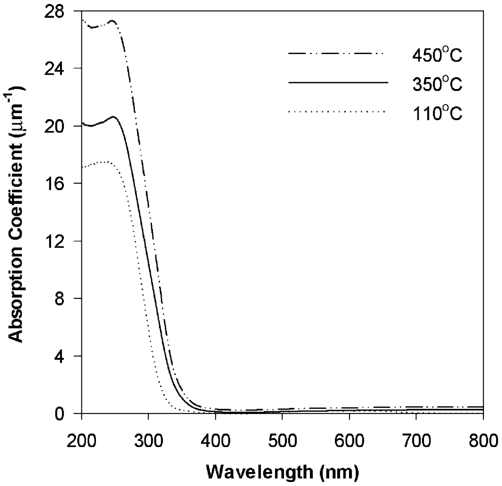

Fig. 4 Absorption spectra of the TiO_2 thin films derived from copolymer templating and then thermally annealed at 110°C, 350°C and 450°C, respectively

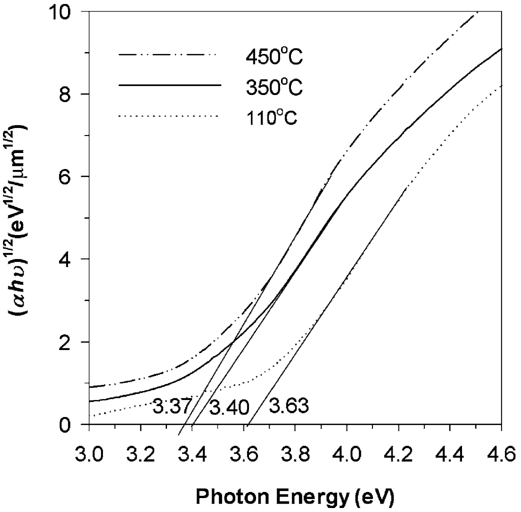

Fig. 5 Plots of $(\alpha h\nu)^{1/2}$ vs photo energy for the TiO_2 thin films derived from copolymer templating and then thermally annealed at 110°C, 350°C and 450°C respectively

temperature (Fig. 4), which is ascribed to the enhanced nanocrystallinity with the rise in thermal annealing temperature. The absence of absorption at above 370 nm suggests that the mesoporous TiO_2 films do not scatter much light in the visible region of the spectrum.

Figure 5 plots the change of $(\alpha h\nu)^{1/2}$ against photon energy for the three thin films, where the intercept on X-axis gives a bandgap energy of 3.63, 3.40 and 3.37 eV for the mesoporous thin films annealed at 110°C, 350°C and 450°C, respectively. The blue shift in the region of 0.2–0.4 eV with respect to that of bulk anatase TiO_2 (3.2 eV) is attributed to the quantum size effect arising from the TiO_2 nanocrystallites. Moreover, the bandgap decreases with increasing temperature, due to the increase in crystallite size, which agrees well with what have been revealed from TEM studies and Raman spectra. For TiO_2 thin films, a large bandgap gives rise to an enhanced redox behavior, suggesting the potential of the mesoporous titania thin films of nanocrystallinity as an effective photocatalyst.

4 Conclusions

Highly ordered mesoporous TiO_2 thin film has been successfully synthesized via a sol-gel route using amphiphilic triblock copolymer as the template in acid media. Evolution of pore configuration and change in nanocrystallinity with increasing annealing temperature were characterized using TEM/HRTEM and Raman spectrophotometry. The mesophases underwent a configuration change from hexagonal, to cubic, and then to a channel-like structure with increasing temperature from 110 to 450°C, in association with the removal of copolymer template and subsequent crystallization of the anatase framework. There is a corresponding red shift in absorption edge, together with a decrease in bandgap energy, with increasing thermal annealing temperature. The observed blue shift in UV-vis absorption edge suggests that the size-quantization effect occurs in the mesoporous TiO_2 thin films.

Acknowledgment This work is supported by the National University of Singapore (R284-000-027-112).

References

1. C.T. Kresge, M.E. Leonowicz, W.J. Roth, J.C. Vartuli, and J.S. Beck, *Nature*, **359**, 710 (1992).
2. J.S. Beck, J.C. Vartuli, W.J. Roth, M.E. Leonowicz, C.T. Kresge, K.D. Schmitt, C.T.W. Chu, D.H. Olson, E.W. Sheppard, S.B. McCullen, J.B. Higgins, and J.L. Schenkler, *J. Am. Chem. Soc.*, **114**, 10835 (1992).
3. Q. Huo, D.I. Margolese, U. Ciesla, D.G. Demuth, P. Feng, T.E. Gier, P. Sieger, A. Firouzi, B.F. Chmelka, F. Schuth, and G.D. Stucky, *Chem. Mater.*, **6**, 1176 (1994).
4. Q. Huo, R. Leon, P.M. Petroff, and G.D. Stucky, *Science*, **268**, 1324 (1995).
5. Q. Huo, D.I. Margolese, and G.D. Stucky, *Chem. Mater.*, **8**, 1147 (1996).
6. D. Grosso, G.J. Soler-Illia, F. Babonneau, C. Sanchez, P.A. Albouy, A. Brunet-Bruneau, and A.R. Balkenende, *Adv. Mater.*, **13**, 1085 (2001).
7. X.S. Li, G.E. Flyxell, J.C. Birnbaum, and C. Wang, *Langmuir*, **20**, 9095 (2004).
8. M. Gratzel, *Curr. Opin. Colloid Interface Sci.*, **4**, 314 (1999).
9. M. Gratzel, *Prog. Photovoltaics: Res. Appl.*, **8**, 171 (2000).
10. A. Hagfeldt and M. Graztel, *Acc. Chem. Res.*, **33**, 269 (2000).
11. L. Kavan, A. Attia, F. Lenzmann, S.H. Elder, and M. Gratzel, *J. Electrochem. Soc.*, **147**, 2897 (2000).
12. M.R. Hoffmann, S.T. Martin, W.Y. Choi, and D.W. Bahnemann, *Chem. Rev.*, **95**, 69 (1995).
13. E.L. Crepaldi, G.J. Soler-Illia, D. Grosso, and C. Sanchez, *New J. Chem.*, **27**, 9 (2003).
14. M.S. Wainwright and N.R. Foster, *Catalysis Rev. Sci. Eng.*, **19**, 211 (1979).